ARTICLE

ACS chemical biology

Development of GlcNAc-Inspired Iminocyclitiols as Potent and Selective *N*-Acetyl-β-Hexosaminidase Inhibitors

Ching-Wen Ho[†,‡,§], Shinde D. Popat[†], Ta-Wei Liu[†], Keng-Chang Tsai[∥], Meng-Jung Ho[†,⊥], Wei-Hung Chen[†], An-Suei Yang[∥,‡], and Chun-Hung Lin[†,∥,‡,⊥,*]

[†]Institute of Biological Chemistry, Academia Sinica, Taipei, Taiwan, [‡]Chemical Biology and Molecular Biophysics, Taiwan International Graduate Program, Academia Sinica, Taipei, Taiwan, [§]Department of Chemistry, National Tsing-Hua University, Hsin-Chu, Taiwan, [∥]The Genomics Research Center, Academia Sinica, Taipei, Taiwan, [⊥]Institute of Biochemical Sciences, National Taiwan University, Taipei, Taiwan

ABSTRACT Human *N*-acetyl-β-hexosaminidase (Hex) isozymes are considered to be important targets for drug discovery. They are directly linked to osteoarthritis because Hex is the predominant glycosidase released by chondrocytes to degrade glycosaminoglycan. Hex is also associated with lysosomal storage disorders. We report the discovery of GlcNAc-type iminocyclitiols as potent and selective Hex inhibitors, likely contributed by the gain of extra electrostatic and hydrophobic interactions. The most potent inhibitor had a K_i of 0.69 nM against human Hex B and was 2.5×10^5 times more selective for Hex B than for a similar human enzyme O-GlcNAcase. These glycosidase inhibitors were shown to modulate intracellular levels of glycolipids, including ganglioside-GM2 and asialoganglioside-GM2.

N-Acetyl-β-hexosaminidase (Hex) is a member of the lysosomal hydrolase family that catalyzes the hydrolysis of terminal, non-reducing *N*-acetyl-β-D-glucosamine (GlcNAc) and *N*-acetyl-β-D-galactosamine (GalNAc) residues in glycoproteins, gangliosides, and glycosaminoglycans (*1, 2*). There are two major Hex isozymes in humans, Hex A and Hex B. Hex A is a heterodimer composed of α and β subunits that are encoded by two related genes, *HEXA* and *HEXB*, respectively. Hex B is a homodimer made up of two identical β-subunits (*3, 4*). Hex S exists as a minor isozyme consisting of two α-subunits. Human Hex isozymes are important because of the role they play in osteoarthritis and lysosomal storage disorders. Hex is the dominant glycosaminoglycan-degrading glycosidase released by chondrocytes into the extracellular milieu. The Hex enzymes are the predominant glycosidases in the synovial fluid from patients with osteoarthritis (*5*). Inhibition of this enzyme can prevent or even reverse cartilage matrix degradation, representing a new avenue in the development of therapeutic treatments for osteoarthritis (*5–7*).

The Hex enzymes are also linked to lysosomal storage disorders that are characterized by the intralysosomal accumulation of glycolipids, including ganglioside-GM2 and asialoganglioside-GM2 (GA2) (*8*). Deficiency of either Hex α- or β-subunit results in clinically devastating neurological diseases. Tay-Sachs disease and Sandhoff disease arise from mutations in *HEXA* and *HEXB*, respectively (*9*). Although enzyme replacement therapy (ERT) has been primarily utilized to treat patients suffering from lysosomal storage disorders, currently there is

***Corresponding author,** chunhung@gate.sinica.edu.tw.

Received for review November 6, 2009 and accepted February 24, 2010.

Published online February 27, 2010

10.1021/cb100011u

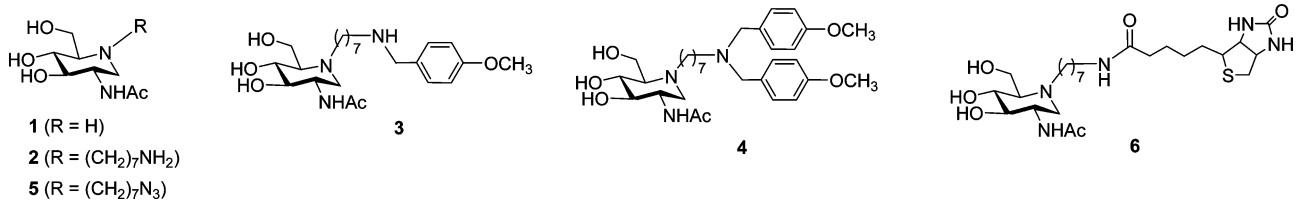

Figure 1. Structures of inhibitors 1−6.

no such treatment for patients with GM2-gangliosidosis (*10*). It is known that ERT is associated with a number of disadvantages, such as extreme high cost and failure to cross the blood−brain barrier, making it necessary to develop other alternatives (*11*). One promising alternative is to use inhibitors of Hex enzymes as pharmacological chaperones (also called chemical chaperones) to increase the stability of defective lysosomal enzymes and thus maintain their metabolic functions at physiologically sustainable levels (*12, 13*). A high-throughput screening was applied to search for drug-like inhibitors, leading to identification of three effective pharmacological chaperones in patient fibroblasts (*13*).

Even though Hex isozymes are suitable targets for drug discovery, currently there are two major challenges to limit their use. The first issue is achieving sufficient inhibitor potency. Second, oftentimes the Hex inhibitors also inhibit a similar enzyme, O-GlcNAcase (an enzyme hydrolyzing terminal GlcNAc residue from O-linked glycoproteins), which uses the same catalytic mechanism (*14, 15*). O-GlcNAcase is categorized in the Glycoside Hydrolase Family 84 based on the CAZy database (*16, 17*), whereas the Hex enzymes are classified in Family 20. In eukaryotic cells, many proteins are modified by O-linked GlcNAc on serine and threonine residues (*18, 19*). The dynamic addition and removal of O-GlcNAc residues requires the action of two essential enzymes, namely, O-GlcNAc transferase (*20, 21*) and O-GlcNAcase, respectively (*22, 23*). A number of inhibitors have been developed to specifically recognize O-GlcNAcase (*14, 24, 25*). Recently the development of potent and selective Hex inhibitors has started to draw attention, such as Gal-PUGNAc by Vocadlo *et al.*, GlcNAc-statins by van Aalten *et al.*, and pyrrolidines by Fleet and co-workers (*26–28*).

Iminocyclitiols have demonstrated great potential in the therapeutic development, as evidenced by *N*-(2-hydroxyethyl)-deoxynojirimycin (Miglitol) for the treatment of type II diabetes. This class of molecules often offers high affinity with glycosidases by providing a good transition-state mimicry at physiological pH. We previously developed 1,5-dideoxy-1,5-imino-L-fucitol derivatives with success by incorporating additional aglycons (groups attached to the iminocyclitol ring) to generate potent and selective inhibitors against α-fucosidase (*29–31*). We sought to determine if iminocyclitol derivatives designed in this study such as 2-acetamido-1,2,5-trideoxy-1,5-imino-D-glucitols (GlcNAc-type iminocyclitiols including compound **1** and related analogues, see Figure 1) are potent inhibitors of Hex, as well as what chemical modifications are able to afford selectivity to distinguish between Hex and O-GlcNAcase. The structure information of human Hex B (*32*) reveals that the vicinity of the enzyme active site contains multiple negative charges. This feature is, nevertheless, not found in the structure of O-GlcNAcase (*15*). Our strategy is thus to incorporate various groups to the ring nitrogen of compound **1** to acquire additional electrostatic and other interactions. The most potent inhibitor was uncovered to show a K_i of 0.69 nM against human Hex B and a K_i of 2.1 nM against Hex A. The inhibition was 2.5×10^5 times more selective for Hex B than for a similar human enzyme O-GlcNAcase. The inhibitors were shown to cause the accumulation of gangliosides GM2 and GA2 by inhibiting lysosomal Hex isozymes, whereas a similar dosage did not affect the level of O-GlcNAc-modified proteins.

RESULTS AND DISCUSSION

We initially synthesized compound **1** (Figure 1) by modification of Vasella's procedure (scheme S1A) (*33–39*). Our modified synthesis has two advantages. The starting material (GlcNAc) to synthesize compound **1** is available at a large scale and low cost. The procedure allows the flexibility of either incorporating any substituent to the ring nitrogen (Supplementary Scheme S1A) or modifying the *N*-acyl group at C2 position (*i.e.*,

TABLE 1. Inhibition constants and selectivity ratios of inhibitors 1–6 for human Hex B and human O-GlcNAcase[a]

	K_i of O-GlcNAcase (μM)	K_i of Hex B (μM)	Selectivity ratio ($K_{i\ O\text{-}GlcNAcase}/K_{i\ Hex\ B}$)
1	23.6 ± 0.97	0.54 ± 0.25	43
2	107.7 ± 9.17	0.0021 ± 0.00038	51,000
3	101.5 ± 6.47	0.0012 ± 0.00023	85,000
4	175.6 ± 2.15	0.00069 ± 0.000077	250,000
5	155.1 ± 9.87	1.7 ± 0.56	91
6	145.0 ± 1.77	0.0267 ± 0.00111	5,400

[a]Values are the means of three determinations ± SD.

the *N*-acetyl group can be hydrolyzed before the final deprotection, followed by acylation).

The enzyme activity was assayed by using 4-methylumbelliferyl *N*-acetylglucosamine (MUG) as the substrate. Hex A was separated from other Hex isozymes by the known procedure (Supplementary Figure S1), and so was Hex B (*40*). In consistence with the previous result (*33*), compound **1** is an inhibitor of Hex B (K_i = 0.54 μM).

To acquire additional electrostatic interactions as aforementioned, the ring nitrogen of compound **1** was attached with several aminoalkyl groups of different chain length. The derivative containing *N*-aminoheptyl group (compound **2** in Figure 1) was found to be the most potent. Kinetic analysis indicated that compound **2** is a competitive inhibitor of Hex B (K_i = 2.1 nM).

To compare the selective inhibition between Hex B and O-GlcNAcase, human O-GlcNAcase was prepared for examination (see Supporting Information) (*23, 41*). Compounds **1** and **2** had K_i values of 23.6 and 107.7 μM for human O-GlcNAcase and 0.54 and 0.0021 μM for Hex B, respectively (Table 1). The ratio $K_{i\ O\text{-}GlcNAcase}/K_{i\ Hex\ B}$ revealed that compound **2** is 51,000 times more selective for Hex B than for O-GlcNAcase, whereas compound **1** is only 43 times more selective.

The inhibitory potential of compound **2** was further enhanced by derivatization with a variety of groups including 180 carboxylic acids (for amide bond formation) (*30, 31*) and 40 aldehydes (for reductive amination) that were purchased from commercial sources. Their molecular structures were shown in Supplementary Figure S2. After the reactions were complete, the resulting mixtures were diluted without purification and assayed for the Hex B activity by using MUG as the substrate (please see pages 8 and 9 of Supporting Information for the detailed information). The derivatives from five carboxylic acids (C9, C10, D11, E4 and F4 shown in Supplementary Figure S2) and three aldehydes (A-4a, B-2a and B-3a in Supplementary Figure S2) were found to give more potent inhibition than others (Supplementary Figure S3). These eight molecules were individually prepared, purified, and examined for the inhibition. The most selective and potent inhibitor of Hex B was obtained when compound **2** was coupled with *p*-methoxybenzaldehyde (B-3a) by reductive amination. As a matter of fact, the reaction produced two products including the monosubstituted product **3** and disubstituted product **4**. Their yields were dependent on the amount of $NaBH_3CN$ and the aldehyde in the reaction (Supplementary Scheme S1B). Both compounds **3** and

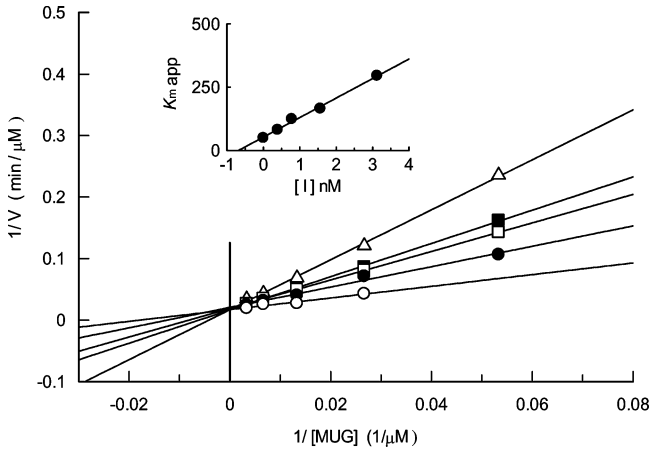

Figure 2. Lineweaver–Burk analysis of Hex B steady-state kinetics in the presence of compound 4. The concentrations of compound 4 used were 3.12 nM (Δ), 1.56 nM (■), 0.78 nM (□), 0.39 nM (●), and 0.00 (○).

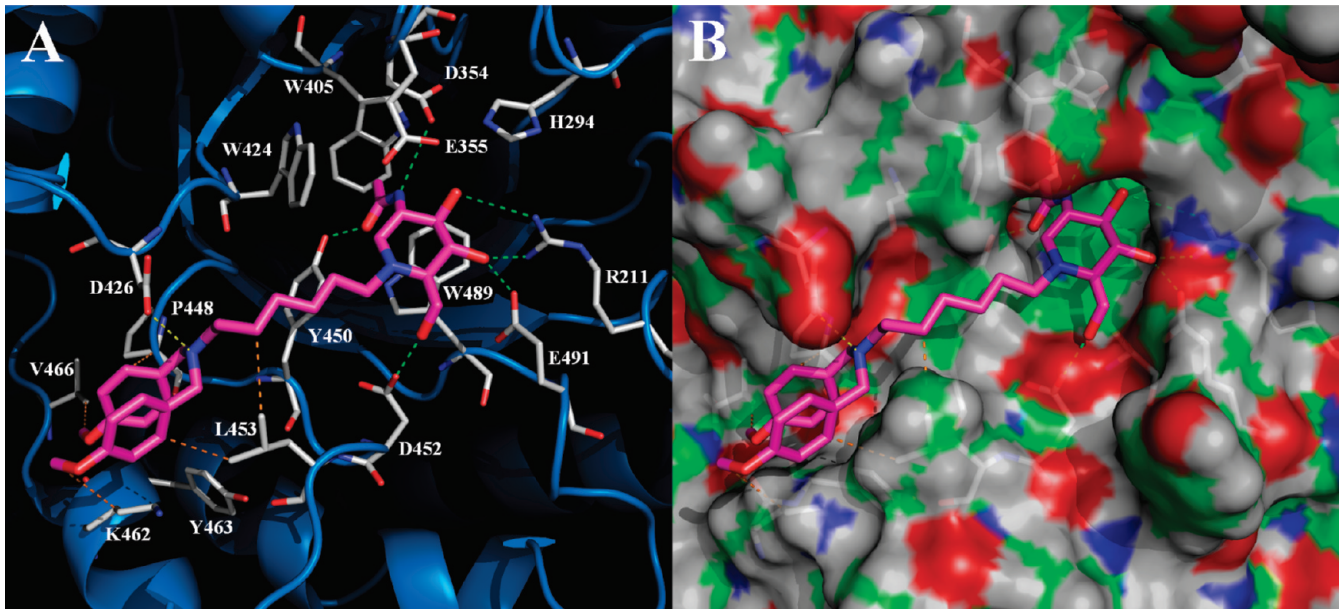

Figure 3. Computational molecular models of inhibitor 4 in the active site of human Hex B (PDB code, 1NOW) as shown in ribbon (Hex B) and stick (inhibitor 4) form (A) and with respect to the Hex B surface (B). The carbon atoms of inhibitor 4 are colored in magenta. The green, orange, and yellow dotted lines represent tentative hydrogen bonding donor−acceptor pairs, hydrophobic, and electrostatic interactions of inhibitor 4 with Hex B, respectively. The molecular models were created using the software PyMOL. A) Side chains of Hex B residues within 7 Å radius centered on inhibitor 4 are also shown in stick explicitly, including carbon (gray), nitrogen (blue), and oxygen (red) atoms. Trace of the Hex B backbone is shown as blue tube. The secondary structure elements are shown in ribbon form, and the important residues involved in inhibitor 4 binding are labeled. B) The colors red, blue, green, and gray on the Hex B surface indicate oxygen, nitrogen, carbon, and hydrogen atoms, respectively.

4 showed greater inhibition of Hex B as compared with compound **2**. In particular, compound **4** had a K_i of 0.69 nM for Hex B and was 250,000 times more selective for Hex B than for O-GlcNAcase (Table 1). Similarly, the same compound exhibited a K_i of 2.1 nM for Hex A. The double reciprocal plot clearly showed compound **4** to be a competitive inhibitor (Figure 2). The chemical modifications from compound **1** to **4** resulted in a significant enhancement in both the potency and selectivity.

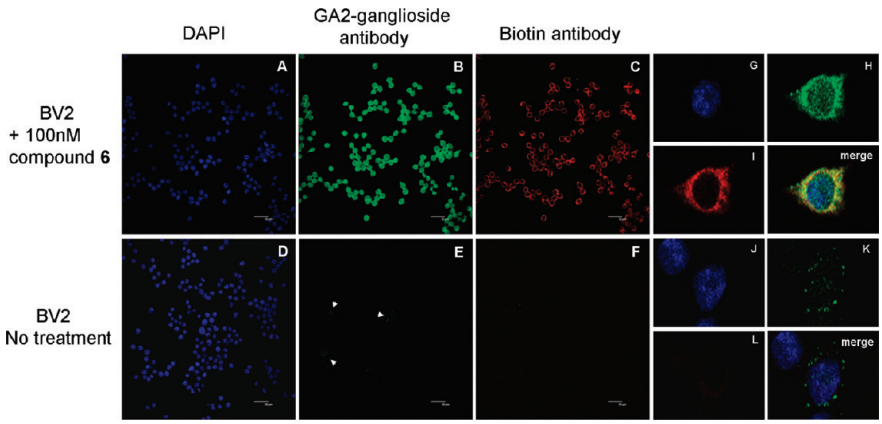

Figure 4. Immunocytochemical analysis of intracellular GA2 ganglioside level. Mouse microglia cells (BV2) cells were cultured in the presence or absence of 100 nM biotin-conjugated inhibitor (6) and then triple stained with polyclonal antibodies against GA2 ganglioside (green, panels B and E), polyclonal antibodies against biotin (red, panels C and F), and 4′,6′-diamidino-2-phenylindole to stain nuclear DNA (blue, panels A and D). GA2 ganglioside accumulated after BV2 was incubated with the inhibitor for 16 h, as shown by significant green fluorescence. The two right-column panels G−L represent higher magnification from selected single cells in panels A−F, respectively. Bars = 30 μm

Meanwhile we also carried out the inhibition study of *Bacteroides fragilis* O-GlcNAcase (Bf O-GlcNAcase, Supplementary Table S1), because the enzyme shares ~40% sequence identity with human homologue. In fact, O-GlcNAcase from a similar strain, *Bacteroides thetaiotaomicrometer* (Bt O-GlcNAcase, showing 74% sequence identity as compared to Bf O-GlcNAcase), was proven highly similar to the human homologue (*15*). The similarity was further corroborated with our inhibition result (Supplementary Table S1) because the inhibition

pattern of Bf O-GlcNAcase is consistent with that of human O-GlcNAcase.

Although the Hex and O-GlcNAcase active sites are structurally similar, the surrounding residues are extremely different. Thus, in principle it would be possible to develop highly selective inhibitors for both Hex and O-GlcNAcase if suitable aglycones could be found. Figure 3 presents a computational modeling analysis of human Hex B (PDB code, 1NOW) in complex with inhibitor **4**. A hydrophobic cleft, enclosed by residues W424, D426, Y450, and L453, is located on the protein surface near the active site; this cleft was found to accommodate the aminoheptyl moiety of inhibitor **4**. The terminal amino group is protonated in solution and likely forms electrostatic interactions with D426, consistent with previous data (*7*). The conversion of the amino group of compound **2** to an azide (compound **5**, shown in Figure 1) not only led to the elimination of the positive charge but also greatly diminished the inhibition up to 810 fold (from K_i = 0.0021 μM of compound **2** to K_i = 1.7 μM of **5**). Additionally, the *p*-methoxybenzyl substituents of inhibitor **4** were surrounded by a hydrophobic pocket composed of residues P448, L450, K462, Y463, and V466. On the other hand, the aglycon of compound **4** [*i.e.*, bis(4-methoxybenzyl)aminoheptyl] could not find a matched pocket in O-GlcNAcase, leading to lower binding affinity with O-GlcNAcase than with Hex A/B.

Because the structure of human O-GlcNAcase is currently unavailable, the X-ray structure of Bt O-GlcNAcase (PDB code, 2J4G) was utilized for the purpose of computational modeling. E355 of human Hex B and D243 of Bt O-GlcNAcase were found to be close to the ring nitrogen of compound **1** at a distance of 3.9 and 4.6 Å, respectively (Supplementary Figure S4-1 and S4-2). The shorter distance in human Hex B may provide compound **1** with a better starting point during optimization of the inhibition selectivity, because the inhibitors **1**−**6** are all more selective for Hex B than for O-GlcNAcase.

To determine if the inhibitors were functional *in vivo*, compound **2** was conjugated with biotin (to give compound **6**, shown in Figure 1) for the purpose of fluorescence imaging and affinity chromatography. Even though the K_i value of compound **6** increased from 2.1 nM (compound **2**) to 26.7 nM, compound **6** was 5400 times more selective for Hex B as compared with O-GlcNAcase. GA2 in mouse microglia cells (BV2) accumulated if the cells were treated with compound **6** (100 nM) for 16 h, as shown in Figure 4, panels A−L. The amount of GA2 was proportional to the concentration of inhibitor **6** and was reached a plateau at 20 nM of inhibitor **6**, as demonstrated by the dot-blot analysis (Supplementary Figure S5). Furthermore, after BV2 cells were treated with compound **1**, **4**, or PUGNAc (200 nM of each) for 10 days, glycosphingolipids were extracted from the cells for analysis of ganglioside level by using high-performance thin-layer chromatography (HP-TLC). Identified by comparison with the authentic standards, GM2 was significantly more increased in the treatment with compound **4** than that with **1** or PUCNAc (Figure 5).

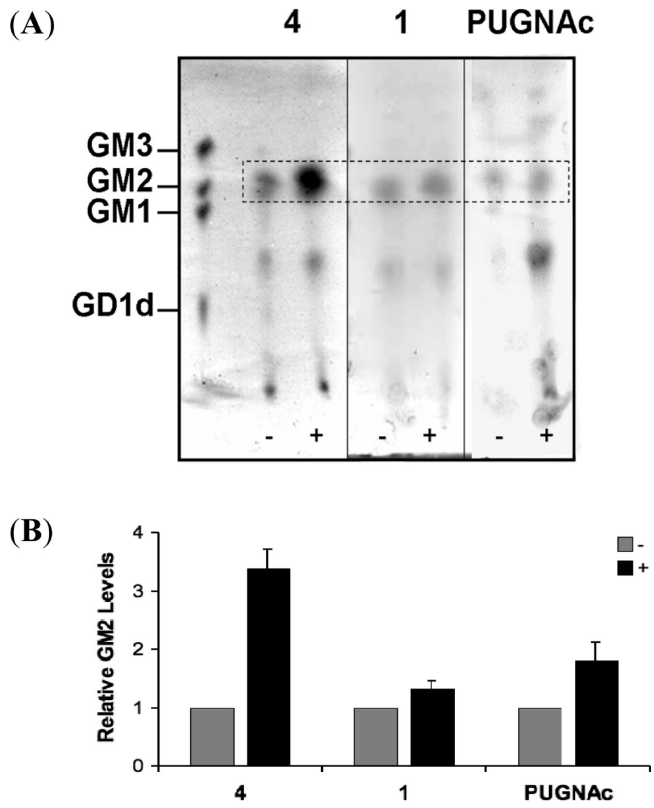

Figure 5. Inhibitors 1, 4, and PUGNAc were shown to increase levels of GM2 in microglia (BV2) cells to a different degree. The cells were treated with 200 nM of each inhibitor for 10 days and extracted with chloroform/methanol for further HP-TLC analysis (A). In each experiment, the control cells (designated as "−") were grown without addition of inhibitor, in parallel to the inhibitor-treated cells (designated as "+"). The spots corresponding to GM2 were further quantified by densitometric analyses (B).

To study the effects of O-GlcNAcase inhibition in human cells, activity of compounds **1**, **2**,and **4** in the human 293T cell line were evaluated by Western blot

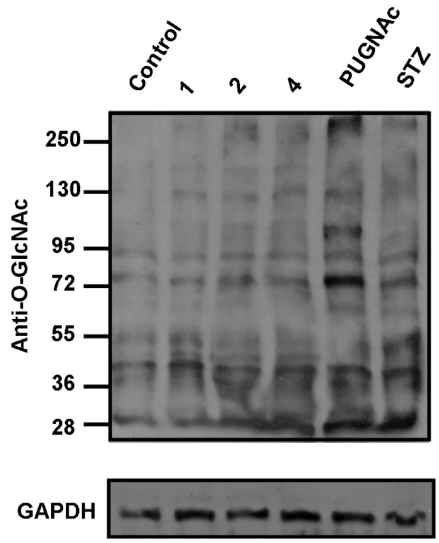

Figure 6. Immunoblot analysis indicated that inhibitors 1, 2, and 4 do not increase the level of O-GlcNAc-modified proteins, in contrast to the two known O-GlcNAcase inhibitors PUGNAc and STZ (positive controls). 293T cells were treated with 10 μM of each inhibitor for 16 h and analyzed for the level of O-GlcNAc-modified proteins by Western blot (upper panel). In contrast, the level of GAPDH was about equal in each lane (lower panel).

analysis with an anti-O-GlcNAc antibody (*14*). Two known O-GlcNAcase inhibitors, PUGNAc ($K_i = 35$ nM) and STZ ($K_i = 14$ μM), were employed as the positive control (*26, 42–44*). No significant accumulation in O-GlcNAc levels was observed when the human cells was treated with 10 μM of compounds **1**, **2**, and **4** (Figure 6). The results echo those of the previous *in vitro* study that compound **4** is much more selective for Hex A/B than for O-GlcNAcase. Furthermore, the concentration of compound **4** can be increased up to 50 μM without altering the level of O-GlcNAc-modified proteins, in contrast to the enhanced level at 200 μM (Supplementary Figure S6). In accordance with Supplementary Figures S5 and S6, we conclude that compound **4** can display the desirable potency and selectivity for Hex B at the range of 20 nM−50 μM without affecting the O-GlcNAcase activity.

There are several strategies to enhance the potency and selectivity of enzyme inhibitors, such as acquisition of additional interaction and better mimicry of the transition state. Our previous development of α-fucosidase inhibitors, for instance, incorporated an extra aglycon to the iminocyclitol, resulting in >1000-fold enhancement in the binding affinity (*29*). The observed enhancement in the potency and selectivity was also documented in the successful development of several potent and selective O-GlcNAcase inhibitors, including PUGNAc pentanamide (*45*), GlcNAcstain (*24*), and NAG-thiazoline derivatives (*14, 25*), where a hydrophobic aglycone and/or *N*-acyl group play a critical role (*45*). A review was recently published that covers the O-GlcNAcase inhibitors in depth (*46*). With respect to Hex inhibitors, the single change in the configuration from PUGNAc to Gal-PUGNAc successfully distinguished between Hex A/B and O-GlcNAcase (*28*). Fleet's, Nitoda's, and Wong's groups also prepared pyrrolidines to give potent inhibition against Hex (*6, 27, 47*). GlcNAcstain was also modified to give nanomolar inhibitors against Hex A/B and O-GlcNAcase (*26*). Recently the 2-acetamino-1,2-dideoxynojirimycin derivatives not only were reported as Hex inhibitors but also utilized to enhance the impaired Hex activity in adult Tay-Sachs and infantile Sandhoff cell lines (*48*). Our synthesized GlcNAc-type iminocyclitiols can significantly improve the potency and selectivity by gaining extra electrostatic and hydrophobic interactions.

Summary and Significance. GlcNAc-type iminocyclitiols were developed and optimized for the Hex inhibition by incorporating various groups to the ring nitrogen of compound **1**. Among the derived products, the best inhibitor (compound **4**) is highly selective for Hex A ($K_i =$ 2.1 nM) and Hex B ($K_i = 0.69$ nM), while it inhibits O-GlcNAcase only at much higher level ($K_i = 175$ μM). The inhibitor was shown to increase GM2- and GA2-ganglioside levels in cultured cells but not affect the level of O-GlcNAc-modified proteins. The result is promising for further development of therapeutic agents for various Hex-related diseases.

METHODS

Synthesis of Compounds 2–4. Due to space limitation, the synthesis and characterization of compounds **1**, **5** and **6** are available in Supporting Information. See Schemes S1A and S1B for the synthetic schemes. Unless otherwise mentioned, all the reactions were conducted using anhydrous solvents under an argon atmosphere. Analytical TLC was performed on precoated plates (Merck, Kieselel 60 F_{254}) with a 250-μm layer thickness.

Flash column chromatography was carried out with silica gel Mallinckrodt Type 60 (230−400 mesh). Reagents of the highest purity were purchased from Sigma and Acros. ^1H and ^{13}C NMR spectra were recorded on 400-MHz instruments with $CDCl_3$ [δ_H 7.26, δ_C 77.0 (central line of a triplet)] or CD_3OD [δ_H 3.30 (central line of a quintet), δ_C 49.0 (central line of a quintet)] as the internal standard. Optical rotations were measured on a digital polarimeter with a cuvette of 10 cm length at ambient temperature.

***N*-[1(7-Amino-heptyl)]-2-acetamido-1,2,5-trideoxy-1,5-imino-D-glucitol (2).** Compound **15** (see Supplementary Scheme S1A; 50.0 mg, 0.08 mmol) was deprotected by hydrogenolysis to generate 18.4 mg of compound 2 in 71% yield. $[\alpha]^{20}_D = +1.50$ (*c* 0.12, MeOH); ^1H NMR (400 MHz, CD_3OD) δ 3.89−3.99 (m, 3H, H-6, H-2), 3.52 (dd, *J* = 9.3, 9.1 Hz, 1H, H-4), 3.43 (dd, *J* = 9.9, 9.2 Hz, 1H, H-3), 3.22 (dd, *J* = 11.6, 4.4 Hz, 1H, H-1equa.), 3.05−3.09 (m, 1H, H-7), 2.96 (t, *J* = 7.5 Hz, 2H, H-13), 2.78−2.84 (m, 1H, H-7), 2.53−2.60 (m, 1H, H-5), 2.51 (dd, *J* = 11.6, 11.1 Hz, 1H, H-1axial), 2.01 (s, 3H, Ac), 1.60−1.70 (m, 4H), 1.39−1.47 (m, 6H); ^{13}C NMR (135 MHz, CD_3OD) δ 173.88, 76.53, 71.79, 67.78, 58.48, 54.52, 53.49, 51.15, 40.85, 30.69, 28.46, 27.77, 27.15, 25.14, 22.93; HRMS (FAB) *m*/*z* calcd for $C_{15}H_{32}N_3O_4$ ($M + H^+$) 318.2393, found 318.2363.

Compound 3. 4-Methoxybenzaldehyde (5.15 mg, 0.038 mmol) was added to a solution of compound **2** (10.0 mg, 0.032 mmol) in methanol (2 mL), as shown in Supplementary Scheme S1B. $NaBH_3CN$ (6.0 mg, 0.096 mmol) was then added slowly to the solution. The resulting mixture was stirred for 36 h at RT. After evaporation to remove the reaction solvent, the residue was purified by silica gel column chromatography with $CHCl_3$/MeOH/NH_4OH (6:3.5:0.5) to give 8.2 mg of product **3** as a colorless syrup at 60% yield. $[\alpha]^{20}_D = +3.00$ (*c* 0.001, MeOH); ^1H NMR (400 MHz, CD_3OD) δ 7.43 (d, *J* = 8.6 Hz, 2H), 7.01 (d, *J* = 8.6 Hz, 2H), 4.14 (s, 2H), 3.88−4.01 (m,3H, H-6, H-2), 3.83 (s, 3H,-OCH_3), 3.52 (t, *J* = 9.4 Hz, 1H, H-3), 3.28−3.40 (m, 2H, H-4, H-1equa.), 3.10−3.17(m, 1H, H-7), 3.06 (t, *J* = 7.9 Hz, 2H, H-13), 2.77−2.84(m, 1H, H 7), 2.41−2.60 (m, 2H, H-5, H-1axial), 1.99 (s, 3H, Ac), 1.61−1.74 (m, 4H), 1.32−1.45 (m, 6H); ^{13}C NMR (135 MHz, CD_3OD) δ 173.91, 162.35, 132.65 (2C), 124.51, 115.74 (2C), 76.42, 71.53, 67.92, 56.01, 54.36, 53.63, 52.05 (2C), 50.88, 46.78, 29.89, 27.84, 27.52, 27.14, 25.31, 22.86; HRMS (FAB) *m*/*z* calcd for $C_{23}H_{40}N_3O_5$ ($M + H^+$) 438.2968, found 438.2958.

Compound 4. 4-Methoxybenzaldehyde (54.0 mg, 0.38 mmol) was added to a solution of compound **2** (30.0 mg, 0.095 mmol) in methanol. $NaBH_3CN$ (27.0 mg, 0.39 mmol) was then slowly added to the solution, as shown in Supplementary Scheme S1B. After stirring at RT for 36 h, the reaction mixture was evaporated and purified by silica gel column chromatography with $CHCl_3$/MeOH (3:1) to give 34.2 mg of compound **4** as a colorless syrup at 65% yield. $[\alpha]^{20}_D = +3.75$ (*c* 0.0016, MeOH); ^1H NMR (400 MHz, CD_3OD) δ 7.27 (d, *J* = 8.5 Hz, 4H), 6.91 (d, *J* = 8.5 Hz, 4H), 3.83−3.88 (m, 3H, H-6, H-2), 3.80 (s, 6H, -OCH_3), 3.61 (bs, 4H, N−CH_2), 3.42 (t, *J* = 9.1, 1H, H-3), 3.23 (dd, *J* = 10.0, 9.0 Hz, 1H, H-4), 3.04 (dd, *J* = 11.3, 4.4 Hz, 1H, H-1equa.), 2.77−2.84 (m, 1H, H-7), 2.47−2.57 (m, 3H, H-7, H-13), 2.10−2.19 (m, 2H, H-5, H-1axial), 1.98 (s, 3H, Ac), 1.39−1.58 (m, 4H), 1.22−1.32 (m, 6H); ^{13}C NMR (135 MHz, CD_3OD) δ 173.75, 161.31 (2C), 132.43 (4C), 115.22 (4C), 114.91 (2C), 77.57, 72.66, 67.67, 59.55, 58.42 (2C), 55.95 (2C), 55.50, 53.63, 53.48, 51.85, 30.16, 28.41, 28.05, 26.44, 25.65, 22.90; HRMS (FAB) *m*/*z* calcd for $C_{31}H_{48}N_3O_6$ ($M + H^+$) 558.3543, found 558.3530.

Kinetic Analysis of O-GlcNAcase, Hex A, and Hex B. All kinetics experiments of O-GlcNAcase, Hex A, and Hex B were determined using the fluorogenic substrate MUG (Sigma). Standard reactions of Hex A or Hex B (200 μL) contained 0.06 nM enzyme in 50 mM citric acid, 100 mM NaCl, 0.1% BSA, pH 4.25, and 0.05−1.5 mM substrate in water. The reactions of O-GlcNAcase (200 μL) contained 2.5 nM enzyme in 50 mM NaH_2PO_4, 100 mM NaCl, 0.1% BSA, pH 6.5, and 0.05−1.5 mM substrates in water. All assays were performed in triplicate at 30 °C for 25 min. The O-GlcNAcase activity was measured in a time-dependent manner, in contrast to the measurement of the Hex A (or Hex B) activity where the reaction was stopped by addition of a 5-fold excess quenching buffer (200 mM sodium glycine buffer, pH 10.8). Both enzymes were stable over the time course in their respective buffers (data not shown). Enzyme activity was measured by fluorescence spectroscopy of the release of 4-methylumbelliferone with an excitation wavelength of 360 nm and an emission wavelength of 460 nm. The data were fit to the Michaelis−Menten equation using the software KaleidaGraph to determine the K_m values. (Please see Supporting Information regarding to the preparation and biochemical characterization of Hex A and Hex B)

The K_i values of compounds **1**−**6** were determined using steady-state kinetics where the MUG concentrations were used at 3- to 5-fold K_m values. To give an ideal progress curve, an appropriate enzyme concentration (0.06 nM of Hex and 2.5 nM of O-GlcNAcaes) and inhibitor concentration (0.3 nM−200 μM) were used. The mode of inhibition was verified by the Lineweaver−Burk plot. The K_i values were determined by the double reciprocal plot ($1/V$ vs $1/[S]$) to give an apparent K_m (the K_m value obtained in the presence of inhibitors). The secondary plot was generated by plotting the apparent K_m values as a function of inhibitor concentration. K_i was determined by calculating the negative value of the resulting *x* intercept.

Immunofluorescence Image Analysis. Commercial antibodies used in this study were purchased from Abcam (rabbit antibiotin, rabbit anti-LIMP II, and rabbit anti-GA2), Abnova (mouse anti-GAPDH), and Invitrogen (4′,6′-diamidino-2-phenylindole [DAPI], goat antimouse Alexa Fluor 594, and goat antirabbit Alexa Fluor 488). For immunofluorescence staining (Figure 4), BV2 cells were grown on glass coverslips and fixed in 4% paraformaldehyde for 15 min. Fixed cells were washed briefly with PBS containing 0.5% (v/v) Triton-X100 and stained with antibodies as indicated. Coverslips were mounted with Prolong antifade reagent (Molecular Probes), and each fluorescent dye was imaged using a Leica TCS SP2 Confocal Microscope and Incubation System (Leica, Germany).

Analysis of Ganglioside Levels and O-GlcNAc-Modified Proteins. BV2 cells were cultured for 24 h in 10-cm tissue culture dishes containing DMEM. Experiments were initiated by plating cells onto a 10-cm plate at approximately 10% confluence and adding 0.2−1.0 μM compound **1**, **4**, or PUGNAc. The cells were allowed to approach confluence after 4−5 days and split 1:3 to a 15-cm plate. After another 4−5 days of growth in media containing the tested inhibitors, the cells were grown to approximately 95% confluence. The cells were then washed once with cold PBS and harvested in 15 mL of PBS. The cells were collected by centrifugation at 250 × *g* for 10 min, lysed, and extracted for obtaining gangliosides according to previous procedure (*49*). The resulting samples were subjected to a Folch partition in $CHCl_3$/MeOH/H_2O of 4:2:1 (v:v:v) (*50*–*52*). The upper layer was collected, dried, and redissolved in $CHCl_3$/MeOH of 2:1 (v:v). Later, 1 mL of water was added, followed by centrifugation to remove the upper layer. The lower layer was further extracted by $CHCl_3$/MeOH/0.1%NaCl of 1:10:10 (v/v/v). The resulting mixture (50−60 μg) was then applied on a HP-TLC plate (Merck) along with a total of 1 μg of a mixture of GM1, GM2, GM3, and GD1d (Sigma) as the authentic standards. Analysis and staining for gangliosides was carried out according to previous protocol (*53*). The plate was run in a solvent system consisting of $CHCl_3$/MeOH/H_2O (containing 0.2% $CaCl_2$) of 55:45:10 (v/v/v), followed by staining with $CeSO_4/H_2SO_4$.

Regarding the analysis of O-GlcNAc levels, 293T cells were grown on 6-cm plates and allowed to reach approximately 80% confluence. Cells were incubated with inhibitors **1**, **2**, **4**, PUGNAc, or STZ (10 μM of each) for 16 h, harvested, and lysed as mentioned previously. Levels of O-GlcNAc-modified proteins and GAPDH (glyceraldehyde-3-phosphate dehydrogenase) (as a loading control) were analyzed by Western blots. Briefly, cell pellets were lysed in 200 μL of lysis buffer, sonicated, and centrifuged to remove cell debris. The cleared cell lysates were then separated by SDS−PAGE, blotted, and probed for levels of *O*-GlcNAc-modified proteins and GAPDH.

Acknowledgment: This work was supported by National Science Council (NSC 97-2628-M-001-016-MY3 and 95-2113-M-001-027-MY3) and Academia Sinica, Taiwan. The data of mass spectrometric analysis were acquired at the NRPGM Core Facilities for Proteomics and Glycomics, Academia Sinica. We thank Mr. Sue-Ming Chang for his assistance in NMR experiments.

Supporting Information Available: This material is available free of charge *via* the Internet at http://pubs.acs.org.

REFERENCES

1. Winchester, B. G. (1996) Lysosomal metabolism of glycoconjugates, *Subcell. Biochem. 27*, 191–238.
2. Watanabe, K. (1936) Biochemical studies on carbohydrates: XXII. On animal β-*N*-monoacetylglucosaminidase. Preliminary report, *J. Biochem. 24*, 297–303.
3. Mahuran, D., and Lowden, J. A. (1980) The subunit and polypeptide structure of hexosaminidases from human placenta, *Can. J. Biochem. 58*, 287–294.
4. Hou, Y., Tse, R., and Mahuran, D. J. (1996) Direct determination of the substrate specificity of the alpha-active site in heterodimeric β-hexosaminidase A, *Biochemistry 35*, 3963–3969.
5. Shikhman, A. R., Brinson, D. C., and Lotz, M. (2000) Profile of glycosaminoglycan-degrading glycosidases and glycoside sulfatases secreted by human articular chondrocytes in homeostasis and inflammation, *Arthritis Rheum. 43*, 1307–1314.
6. Liu, J., Shikhman, A. R., Lotz, M. K., and Wong, C. H. (2001) Hexosaminidase inhibitors as new drug candidates for the therapy of osteoarthritis, *Chem. Biol. 8*, 701–711.
7. Liang, P.-H., Cheng, W.-C., Lee, Y.-L., Yu, H.-P., Wu, Y.-T., Lin, Y.-L., and Wong, C.-H. (2006) Novel five-membered iminocyclitol derivatives as selective and potent glycosidase inhibitors: new structures for antivirals and osteoarthritis, *ChemBioChem 7*, 165–173.
8. Gravel, R. A., Clarke, J. T. R., Kaback, M. M., Mahuran, D., Sandoff, K., and Suzuki, K. (1995) The Metabolic and Molecular Basis of Inherited Diseases, in *The GM2 Gangliosidoses*, pp 2839−2879, McGraw-Hill, New York.
9. Mahuran, D. J. (1999) Biochemical consequences of mutations causing the GM2 gangliosidoses, *Biochim. Biophys. Acta 1455*, 105–138.
10. Tsuji, D., Kuroki, A., Ishibashi, Y., Itakura, T., and Itoh, K. (2005) Metabolic correction in microglia derived from Sandhoff disease model mice, *J. Neurochem. 94*, 1631–1638.
11. Desnick, R. J., and Schuchman, E. H. (2002) Enzyme replacement and enhancement therapies: lessons from lysosomal disorders, *Nat. Rev. Genet. 3*, 954–966.
12. Tropak, M. B., Reid, S. P., Guiral, M., Withers, S. G., and Mahuran, D. (2004) Pharmacological enhancement of β-hexosaminidase activity in fibroblasts from adult Tay-Sachs and Sandhoff patients, *J. Biol. Chem. 279*, 13478–13487.
13. Tropak, M. B., Blanchard, J. E., Withers, S. G., Brown, E. D., and Mahuran, D. (2007) High-throughput screening for human lysosomal β-*N*-Acetyl hexosaminidase inhibitors acting as pharmacological chaperones, *Chem. Biol. 14*, 153–164.
14. Macauley, M. S., Whitworth, G. E., Debowski, A. W., Chin, D., and Vocadlo, D. J. (2005) O-GlcNAcase uses substrate-assisted catalysis: kinetic analysis and development of highly selective mechanism-inspired inhibitors, *J. Biol. Chem. 280*, 25313–25322.
15. Dennis, R. J., Taylor, E. J., Macauley, M. S., Stubbs, K. A., Turkenburg, J. P., Hart, S. J., Black, G. N., Vocadlo, D. J., and Davies, G. J. (2006) Structure and mechanism of a bacterial β-glucosaminidase having O-GlcNAcase activity, *Nat. Struct. Mol. Biol. 13*, 365–371.
16. Henrissat, B. (1991) A classification of glycosyl hydrolases based on amino acid sequence similarities, *Biochem. J. 280*, 309–316.
17. Henrissat, B. (1991) Sequence homology between a β-galactosidase and some β-glucosidases, *Protein Sequences Data Anal. 4*, 61–62.
18. Torres, C. R., and Hart, G. W. (1984) Topography and polypeptide distribution of terminal *N*-acetylglucosamine residues on the surfaces of intact lymphocytes. Evidence for O-linked GlcNAc, *J. Biol. Chem. 259*, 3308–3317.
19. Kamemura, K., Hayes, B. K., Comer, F. I., and Hart, G. W. (2002) Dynamic interplay between O-glycosylation and O-phosphorylation of nucleocytoplasmic proteins: alternative glycosylation/phosphorylation of THR-58, a known mutational hot spot of c-Myc in lymphomas, is regulated by mitogens, *J. Biol. Chem. 277*, 19229–19235.
20. Lubas, W. A., Frank, D. W., Krause, M., and Hanover, J. A. (1997) O-Linked GlcNAc transferase is a conserved nucleocytoplasmic protein containing tetratricopeptide repeats, *J. Biol. Chem. 272*, 9316–9324.
21. Kreppel, L. K., Blomberg, M. A., and Hart, G. W. (1997) Dynamic glycosylation of nuclear and cytosolic proteins. Cloning and characterization of a unique O-GlcNAc transferase with multiple tetratricopeptide repeats, *J. Biol. Chem. 272*, 9308–9315.
22. Dong, D. L., and Hart, G. W. (1994) Purification and characterization of an O-GlcNAc selective *N*-acetyl-β-D-glucosaminidase from rat spleen cytosol, *J. Biol. Chem. 269*, 19321–19330.
23. Gao, Y., Wells, L., Comer, F. I., Parker, G. J., and Hart, G. W. (2001) Dynamic O-glycosylation of nuclear and cytosolic proteins: cloning and characterization of a neutral, cytosolic β-*N*-acetylglucosaminidase from human brain, *J. Biol. Chem. 276*, 9838–9845.
24. Dorfmueller, H. C., Borodkin, V. S., Schimpl, M., Shepherd, S. M., Shpiro, N. A., and van Aalten, D. M. (2006) GlcNAcstatin: a picomolar, selective O-GlcNAcase inhibitor that modulates intracellular O-glcNAcylation levels, *J. Am. Chem. Soc. 128*, 16484–16485.
25. Yuzwa, S. A., Macauley, M. S., Heinonen, J. E., Shan, X., Dennis, R. J., He, Y., Whitworth, G. E., Stubbs, K. A., McEachem, E. J., Davies, G. J., and Vocadlo, D. J. (2008) A potent mechanism-inspired O-GlcNAcase inhibitor that blocks phosphorylation of tau *in vivo*, *Nat. Chem. Biol. 4*, 483–490.
26. Dorfmueller, H. C., Borodkin, V. S., Schimpl, M., and van Aalten, D. M. F. (2009) GlcNAcstatins are nanomolar inhibitors of human O-GlcNAcase inducing cellular hyper-O-GlcNAcylation, *Biochem. J. 420*, 221–227.
27. Rountree, J. S., Butters, T. D., Wormald, M. R., Boomkamp, S. D., Dwek, R. A., Asano, N, Ikeda, K., Evinson, E. L., Nash, R. J., and Fleet, G. W. (2009) Design, synthesis, and biological evaluation of enantiomeric β-*N*-acetylhexosaminidase inhibitors LABNAc and DABNAc as potential agents against Tay-Sachs and Sandhoff disease, *ChemMedChem 4*, 378–392.
28. Stubbs, K. A., Macauley, M. S., and Vocadlo, D. J. (2009) A selective inhibitor Gal-PUGNAc of human lysosomal β-Hexosaminidases modulates levels of the ganglioside GM2 in neuroblastoma cells, *Angew. Chem., Int. Ed. 48*, 1300–1303.
29. Ho, C. W., Lin, Y. N., Chang, C. F., Li, S. T., Wu, Y. T., Wu, C. Y., Liu, S. W., Li, Y. K., and Lin, C. H. (2006) Discovery of different types of inhibition between the human and thermotoga maritima α-fucosidases by fuconojirimycin-based derivatives, *Biochemistry 45*, 5695–5702.

30. Chang, C.-F., Ho, C.-W., Wu, C.-Y., Chao, T.-A., Wong, C.-H., and Lin, C.-H. (2004) Discovery of picomolar slow tight-binding inhibitors of α-fucosidase, *Chem. Biol. 11*, 1301–1306.
31. Wu, C.-Y., Chang, C.-F., Chen, J.-S., Wong, C.-H., and Lin, C.-H. (2003) Rapid diversity-oriented synthesis in microtiter plates for *in situ* screening: discovery of potent and selective α-fucosidase inhibitors, *Angew. Chem., Int. Ed. 42*, 4661–4664.
32. Mark, B. L., Mahuran, D. J., Cherney, M. M., Zhao, D., Knapp, S., and James, M. N. (2003) Crystal structure of human β-hexosaminidase B: understanding the molecular basis of Sandhoff and Tay-Sachs disease, *J. Mol. Biol. 327*, 1093–1109.
33. Fleet, G. W. J., Smith, P. W., Nash, R. J., Fellows, L. E., Parekh, R. B., and Rademacher, T. W. (1986) Synthesis of 2-acetamido-1,5-imino-1,2,5-trideoxy-D-mannitol and of 2-acetamido-1,5-imino-1,2,5-trideoxy-D-glucitol, a potent and specific inhibitor of a number of β-*N*-acetylglucosaminidases, *Chem. Lett. 7*, 1051–1054.
34. Kappes, E., and Legler, G. (1989) Synthesis and inhibitory properties of 2-acetamido-2-deoxynojirimycin (2-acetamido-5-amino-2,5-dideoxy-D-glucopyranose, 1) and 2-acetamido-1,2-dideoxynojirimycin (2-acetamido-1,5-imino-1,2,5-trideoxy-D-glucitol, 2), *J. Carbohydr. Chem. 8*, 371–388.
35. Overkleeft, H. S., van Wiltenburg, J., and Pandit, U. K. (1994) A facile transformation of sugar lactones to azasugars, *Tetrahedron 50*, 4215–4224.
36. Overkleeft, H. S., van Wiltenburg, J., and Pandit, U. K. (1993) An expedient stereoselective synthesis of gluconolactam, *Tetrahedron Lett. 34*, 2527–2528.
37. Kajimoto, T., Liu, K. K-C., Pederson, R. L., Zhong, Z., Ichikawa, Y., Porco, J. A., and Wong, C. H. (1991) Enzyme-catalyzed aldol condensation for asymmetric synthesis of azasugars: synthesis, evaluation, and modeling of glycosidase inhibitors, *J. Am. Chem. Soc. 113*, 6187–6196.
38. Furneaux, R. H., Gainsford, G. J., Lynch, G. P., and Yorke, S. C. (1993) 2-Acetamido-1,2-dideoxynojirimycin: an improved synthesis, *Tetrahedron 39*, 9605–9612.
39. Granier, T., and Vasella, A. (1998) Synthesis and some transformations of 2-acetamido-5-amino-3,4,6-tri-*O*-benzyl-2,5-dideoxy-D-glucono-1,5-lactam, *Helv. Chim. Acta 81*, 865–880.
40. Sharma, R., Bukovac, S., Callahan, J., and Mahuran, D. (2003) A single site in human β-hexosaminidase A binds both 6-sulfate-groups on hexosamines and the sialic acid moiety of GM2 ganglioside, *Biochim. Biophys. Acta 1637*, 113–118.
41. Macauley, M. S., Stubbs, K. A., and Vocadlo, D. J. (2005) O-GlcNAcase catalyzes cleavage of thioglycosides without general acid catalysis, *J. Am. Chem. Soc. 127*, 17202–17203.
42. Rao, F. V., Dorfmueller, H. C., Villa, F., Allwood, M., Eggleston, I. M., and van Aalten, D. M. (2006) Structural insights into the mechanism and inhibition of eukaryotic O-GlcNAc hydrolysis, *EMBO J. 25*, 1569–1578.
43. Hanover, J. A., Lai, Z., Lee, G., Lubas, W. A., and Sato, S. M. (1999) Elevated O-linked *N*-acetylglucosamine metabolism in pancreatic β-cells, *Arch. Biochem. Biophys. 362*, 38–45.
44. He, Y., Martinez-Fleites, C., Bubb, A., Gloster, T. M., and Davies, G. J. (2009) Structural insight into the mechanism of streptozotocin inhibition of O-GlcNAcase, *Carbohydr. Res. 344*, 627–631.
45. Whitworth, G. E., Macauley, M. S., Stubbs, K. A., Dennis, R. J., Taylor, E. J., Davies, G. J., Greig, I. R., and Vocadlo, D. J. (2007) Analysis of PUGNAc and NAG-thiazoline as transition state analogues for human O-GlcNAcase: mechanistic and structural insights into inhibitor selectivity and transition state poise, *J. Am. Chem. Soc. 129*, 635–644.
46. Macauley, M. S., and Vocadlo, D. J. (1800) (2010) Increasing O-GlcNAc levels: An overview of small-molecule inhibitors of O-GlcNAcase, *Biochim. Biophys. Acta* 107–121.
47. Usuki, H., Toyo-oka, M., Kanzaki, H., Okuda, T., and Nitoda, T. (2009) Pochonicine, a polyhydroxylated pyrrolizidine alkaloid from fungus *Pochonia suchlasporia* var. suchlasporia TAMA 87 as a potent β-*N*-acetylglucosaminidase inhibitor, *Bioorg. Med. Chem. 17*, 7248–7253.
48. Steiner, A. J., Schitter, G., St,tz, A. E., Wrodnigg, T. M., Tarling, C. A., Withers, S. G., Mahuran, D. J., and Tropak, M. B. (2009) 2-Acetamino-1,2-dideoxynojirimycin-lysine hybrids as hexosaminidase inhibitors, *Tetrahedron: Asymmetry 20*, 832–835.
49. Yowler, B. C., Kensinger, R. D., and Schengrund, C.-L. (2002) Botulinum neurotoxin a activity is dependent upon the presence of specific gangliosides in neuroblastoma cells expressing synaptotagmin I, *J. Biol. Chem. 277*, 32815–32819.
50. Folch, J., Lees, M., and Sloane Stanley, G. H. (1957) A simple method for the isolation and purification of total lipides from animal tissues, *J. Biol. Chem. 226*, 497–509.
51. Stroud, M. R., Levery, S. B., Nudelman, E. D., Salyan, M. E., Towell, J. A., Roberts, C. E., Watanabe, M., and Hakomori, S. (1991) Extended type 1 chain glycosphingolipids: dimeric Lea (III4V4Fuc2Lc6) as human tumor-associated antigen, *J. Biol. Chem. 266*, 8439–8446.
52. Fan, Y. Y., Yu, S. Y., Ito, H., Kameyama, A., Sato, T., Lin, C. H., Yu, L. C., Narimatsu, H., and Khoo, K. H. (2008) Identification of further elongation and branching of dimeric type 1 chain on lactosylceramides from colonic adenocarcinoma by tandem mass spectrometry sequencing analyses, *J. Biol. Chem. 283*, 16455–16468.
53. Kundu, S. K., and John, M. L. (1981) Thin-layer chromatography of neutral glycosphingolipids and gangliosides, *Methods Enzymol. 72*, 185–204.